ELSEVIER

Journal of Photochemistry and Photobiology A: Chemistry 126 (1999) 7–14

Journal of Photochemistry and Photobiology A:Chemistry

www.elsevier.nl/locate/jphotochem

Time dependent solvent effects on the T_1–T_n absorption spectra of thioxanthone: a picosecond investigation

F. Morlet-Savary *, C. Ley, P. Jacques, F. Wieder, J.P. Fouassier

Département de Photochimie Générale, UMR 7525, Ecole Nationale Supérieure de Chimie, 3 rue Alfred Werner, 68093 Mulhouse Cedex, France

Accepted 19 May 1999

Abstract

Time resolved absorption (expressed by the shift of the wavenumber of maximum absorption $\nu_{TT}^{0} \rightarrow \nu_{TT}^{\infty}$) of a probe (thioxanthone) in its triplet state (^{3}TX) is investigated in different solvents, using picosecond absorption experiments. By increasing the solvent polarity, ν_{TT}^{∞} is blue shifted due to a decrease of the dipole moment upon excitation and linearly depends on the empirical polarity parameter $E_T(30)$. Moreover, application of the solvatochromic comparison method (SCM) (π^*, α, β) shows that specific interactions are prevailing in alcohols. On the contrary, ν_{TT}^{0} is red shifted and correlates linearly well with the classical function of the refractive index (n): $2(n^2 - 1)/2n^2 + 1$. In hydroxylic solvents, the solvent response function $C(t)$ is described by a monoexponential τ_{TX}. Comparison of τ_{TX} with other values concerning either probes in the singlet state or solvent characteristic relaxation times underlines the key role of the specific ^{3}TX solvent hydrogen bonding.

Keywords: Thioxanthone; Picosecond; Transient absorption; Solvatochromy; Solvent effects

1. Introduction

Solvent effect is certainly one aspect of physical chemistry which has arisen large interests during the past 3 decades. A great deal of papers were devoted particularly to the displacement of electronic absorption and luminescence spectra (solvatochromic shifts) in relation to the solute medium interaction, a topic recently reviewed [1,2]. This is not surprising since the photophysical and photochemical properties of a molecule are determined by the nature and the energy of its electronically excited states. In this respect, thioxanthone (TX) provides a particular versatile example: among other, its fluorescence maximum wavelength, quantum yield, lifetime are dramatically solvent dependent [3–8]. Moreover, as for the optimization of photosensitive formulations, the study of the interactions between the thioxanthone derivatives and its surrounding may play a very important role.

Coming of lasers empowered photochemists to investigate solvent effects on such important transient species as triplet states. It can be noticed that to obtain a triplet–triplet UV absorption spectrum with a nanosecond equipment was and even still is somewhat tedious. On the contrary picosecond spectroscopy can quickly provide reliable and well resolved transient absorption spectrum. Moreover, this time scale allows an investigation of solvation dynamics. As an example, a detailed study of the T_1–T_n absorption spectrum of TX revealing interesting features especially in hydroxylic solvents is reported here.

2. Experimental part

Picosecond experiments were performed using a classical spectroscopic design. The basic principle consists in preparing a transient species with a short laser pulse (pump pulse) and to pass a white light pulse (probe pulse) through the sample so that an absorption spectrum can be recorded. The picosecond pulses are delivered by a passively-actively mode locked Nd : YAG laser (BM Industries). Both fundamental (1064 nm) and third harmonic (355 nm) emissions were used, respectively, to generate a white light continuum probe from D_2O/H_2O mixture and to excite the sample in solution. The white light is collected and then collimated by a set of achromatic lenses, sent onto a large band beamsplitter to illuminate both sample and reference cells. The transmitted light is focused by appropriate lenses and injected into fiber optics directly connected to the dispersive element (Jobin Yvon CP 200) of the double diode

* Corresponding author.

1010-6030/99/$ – see front matter
PII: S1010-6030(99)00117-3

arrays multichannel analyzer (Princeton Instruments ST 120 controller and DDA1024 detector). The solution is flowed through two cells (2 mm optical pathway), the reference one (nonexcited) and the sample one (excited). A delay of up to 6 ns could be achieved between the pump and probe pulses using a computer controlled micrometer translation stage. The transient absorbance is calculated according to:

$$\mathrm{Abs} = \log\left\{\frac{I^0_{\mathrm{sample}}}{I^0_{\mathrm{ref}}}\frac{I^{\mathrm{e}}_{\mathrm{ref}}}{I^{\mathrm{e}}_{\mathrm{sample}}}\right\}$$

where I^0_{ref} and I^0_{sample} refer to the intensities measured through reference and sample cells with excitation off, $I^{\mathrm{e}}_{\mathrm{ref}}$ and $I^{\mathrm{e}}_{\mathrm{sample}}$ to the ones measured with excitation on. To get a transient absorption spectrum, signals are averaged over 400 laser shots with the excitation beam present followed by another 400 laser shots without the excitation beam. The laser excitation energy is about 250 μJ and the excitation and probe diameters are in 2 and 1 mm, respectively.

The rise of transient absorbance Abs(t, λ_{obs}) obtained from the transient spectra at an observed wavelength λ_{obs} is fitted according to

$$\mathrm{Abs}(t,\ \lambda_{\mathrm{obs}}) = \int_0^t R(\tau)F(t-\tau)\,\mathrm{d}\tau$$

where $R(t)$ is the instrument response function produced by the convolution of the pump and probe pulses and is assumed to have the analytical form of a Gaussian with a pulse width of σ

$$R(t) = \frac{1}{\sqrt{2\pi}\sigma}\exp\left[-\frac{(t-t_0)^2}{2\sigma^2}\right]$$

where t_0 is the position of the peak of the Gaussian. This time t_0 corresponds to the maximum overlap between the pump and probe pulses. Monitoring the risetime of the $S_1 \rightarrow S_n$ absorption for pyrene and anthracene following the 355 nm excitation, the width σ is about 25 ps, the value of t_0 is around 100 ps and wavelength dependent. The risetime of the $T_1 \rightarrow T_n$ absorption for benzophenone in acetonitrile solution is directly related to the intersystem crossing rate constant. The fitting of this risetime yields an experimental value of 10 ± 5 ps in the typical experimental conditions, which is in good agreement with values published elsewhere (9.6 ± 0.9 ps in acetonitrile) [9]. Finally, this experimental value can be considered as the resulting time resolution of the experimental set-up and is estimated to be better than 10 ps. Fortunately, it was possible to investigate the T_1–T_n spectrum in a sufficient number of solvents to extricate clear trends in the solvent effects.

3. Results and discussion

It is well-known that following light excitation, TX undergoes a rapid intersystem crossing towards the triplet state [10]. Fig. 1 shows the T_1–T_n absorption in 1-butanol. It should be noted that this absorption spectrum is nearly free of noise which enables the location of the maximum with much better precision than with nanosecond laser spectroscopy. Moreover, it appears that the absorption maximum evolves with time towards shorter wavelengths. It is, therefore, convenient to define two distinct wavenumbers of maximum absorption for the T_1–T_n absorption spectrum as reported in Fig. 1. One corresponds to the growing up of the triplet state just after light excitation (ν^0_{TT}). The second one (ν^∞_{TT}) corresponds to the wavenumber of the T_1–T_n spectrum observed once all the solute/solvent interactions are effective.

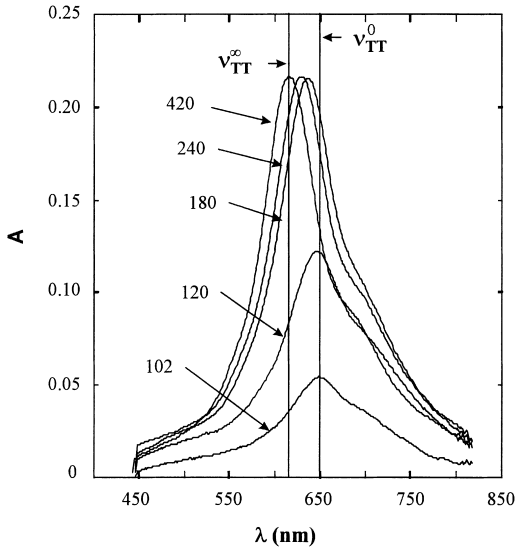

Fig. 1. Blue shift ($\Delta\nu = 775°\mathrm{cm}^{-1}$) of the T–T absorption in 1-butanol. ν^0_{TT} corresponds to the extrapolated maximum at time $t = 0$ which is evaluated to be $\lambda_{\mathrm{max}} = 648$ nm. ν^∞_{TT} corresponds to the maximum ($\lambda_{\mathrm{max}} = 617$ nm) observed after relaxation of the solvent and total influence of the hydrogen bond specific interactions ($t = \infty$). Intermediate times in picoseconds.

Thorough description of solute/solvent interactions is a many-faceted topic for which the level of approach needs a distinction between normal and specific interactions. Normal solute/solvent interactions involve only multipole and polarisability properties of the solute and solvent molecules. They can be satisfactorily treated in the frame of the dielectric continuum model. This model characterizes the solvent by its static dielectric constant (D), its refractive index (n) and the Onsager polarity functions.

$$f(D) = \frac{2(D-1)}{2D+1} \tag{1}$$

$$f(n^2) = \frac{2(n^2-1)}{2n^2+1} \tag{2}$$

The overall solvatochromic shift results from the four following differences of solvation energy [1] between a relaxed initial state (with dipole moment $\vec{\mu}_{\mathrm{g}}$ in absorption) and a Franck–Condon final state ($\vec{\mu}_{\mathrm{e}}$ in absorption) from Solvent 1 to Solvent 2:

Dipole – dipole interaction:

$$(\Delta E_{ge})_{1-2} = -\vec{\mu}_g(\vec{\mu}_e - \vec{\mu}_g)a^{-3}[f(D) - f(n^2)]_{1-2} \quad (3)$$

Solute dipole – solvent polarisability:

$$(\Delta E_{ge})_{1-2} = -(\mu_e^2 - \mu_g^2)(2a)^{-3}[f(n^2)]_{1-2} \quad (4)$$

Solute polarisability – solvent dipole:

$$(\Delta E_{ge})_{1-2} = -(\alpha_e - \alpha_g)a^{-3}L[f(D) - f(n^2)]_{1-2} \quad (5)$$

Polarizability – polarisability:

$$(\Delta E_{ge})_{1-2} = -(\alpha_e - \alpha_g)a^{-3}C[f(n^2)]_{1-2} \quad (6)$$

μ_g and μ_e are the dipolar moments of the relaxed initial state and Franck–Condon final state respectively of the solute, α_g and α_e are the polarisability of the ground and excited states respectively of the solute, a the radius of the solute considered as a sphere and L and C are scaling factors.

A complete description of the solvatochromic effects would need the introduction of one more term. It is related to the transition dipole moment (M) which inevitably accompanies the electronic transition of the solute molecule and describes the motion of electrical charges during the transition. The corresponding solvatochromic shift can be expressed as Eq. (7). However, its contribution is negligible [1] and this term will not be considered hereafter.

$$(\Delta E_{ge})_{1-2} = -\left(\frac{M^2}{2a^3}\right) f(n^2)_{1-2} \quad (7)$$

At this stage, it is important to note that the refractive index is present in the four relations Eqs. (3)–(6) to be considered.

The above mentioned relations totally exclude specific interactions such as hydrogen bonds. Therefore, in the case of hydroxylic solvents, the 'empirical' methods must be considered. Among the plethoric methods which aim to determine an empirical polarity parameter of the solvents, two well-known approaches were chosen: (i) the totally empirical method which describes all the solvent/solute interactions using only one parameter $E_T(30)$. This parameter is based on the UV transition energy of a betaine dye and is certainly the most famous [11], (ii) the semi-empirical method, in fact a multilinear approach called solvatochromic comparison method (SCM) [12]. The SCM method aims to unravel, quantify, correlate and rationalize all the solvent/solute interactions. This method was intended for use in linear solvation energy relationships (LSERs):

$$XYZ = XYZ_0 + s\pi^* + a\alpha + b\beta \quad (8)$$

where XYZ and XYZ_0 are the investigated properties in the solvent and gas phase, respectively; π^* is an index of solvent dipolarity/polarisability which measures the ability of the solvent to stabilize a charge or a dipole by virtue of its dielectric effect; α describes the ability of the solvent to give a proton in a solvent to solute hydrogen bond and β provides a measure of the ability of the solvent to accept a proton in a solute to solvent hydrogen bond. The field of applications and details concerning these methods can be found in the following references [1,11,12].

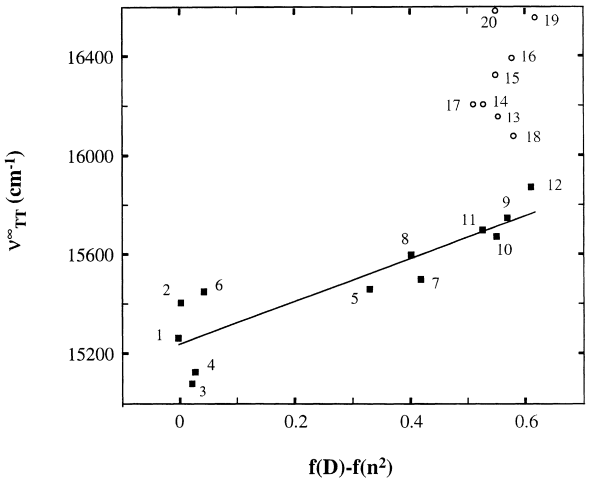

Fig. 2. Failure of the dielectric continuum model to explain the shift of ν_{TT}^{∞}.Nonpolar and polar solvents (■), hydroxylic solvents (○). The line relies ν_{TT}^{∞} to $[f(D) - f(n^2)]$ for nonhydroxylic solvents.

For the present purpose, it is sufficient to say that with the help of these methods and depending on the chemical nature of the solvents considered, the solvent effects on ν_{TT}^{∞}, ν_{TT}^{0} reported in Table 1 can be explained.

3.1. Relaxed ^{3}TX solvatochromy (ν_{TT}^{∞})

The transition occurs from a totally relaxed T_1 state towards an upper state T_n (Franck–Condon state). This corresponds to a classical solvatochromic study and was indeed already investigated for thioxanthone using nanosecond spectroscopy [6]. The T_1–T_n absorption spectrum is blue shifted, as the polarity increases (see Table 1) indicating a decrease in the dipole moment upon excitation. The dipole moment of the ground state was recently measured $\mu_{S0} = 2.65$ D [16]. From the analyses of the data performed according to the treatment proposed by BILOT and KAWSKI and reported in reference [6], the following values can be extracted: $\mu_{s1} = 4.9$ D; $\mu_{T1} = 4.9$ D; $\mu_{Tn} = 3.4$ D. Therefore, the decrease of the dipole moment of the present probe $\Delta\mu_{TT} = -1.5$ D is moderate compared to the dramatic increase $\Delta\mu_{SS} \sim 10$ D observed for a common probe, coumarin 153 [17].

Moreover, it can be seen from Fig. 2 that the dielectric continuum model fails to explain the shift when taking into account all the solvents. It is possible to find a linear relation between ν_{TT}^{∞} and Onsager's polarity function $[f(D) - f(n^2)]$, only for nonhydroxilic solvents.

On the contrary, it appears from Fig. 3 that $E_T(30)$ can give account of the T_1–T_n shift for all the solvents investigated here (i.e., including the hydroxylic solvents). The following linear correlation relies ν_{TT}^{∞} to the $E_T(30)$ parameter:

Table 1
Experimental data and solvent parameters $E_T(30)$ from [13] except triethyleneglycol (No. 20) from [14]; n, D from [15]; p^*, α from [13]

No.	Solvent	λ_{TT}^0 (nm)	λ_{TT}^∞ (nm)	ν_{TT}^0 (cm^{-1})	ν_{TT}^∞ (cm^{-1})	$E_T(30)$	π^*	a	n	D	$f(n^2)$	$f(D)-f(n^2)$
1	cyclohexane	655	655	15267	15267	30.9	0.00	0.00	1.426	2.024	0.408	−0.002
2	n-hexane	649	649	15408	15408	31.0	−0.04	0.00	1.372	1.886	0.371	0.001
3	CCl_4	663	663	15083	15083	32.4	0.28	0.00	1.460	2.237	0.430	0.022
4	toluene	661	661	15129	15129	33.9	0.54	0.00	1.497	2.380	0.453	0.027
5	ether	647	647	15463	15463	34.5	0.27	0.00	1.353	4.267	0.356	0.329
6	dioxane	647	647	15455	15455	36.0	0.55	0.00	1.422	2.219	0.406	0.043
7	THF	645	645	15503	15503	37.4	0.48	0.00	1.405	7.520	0.394	0.813
8	ethylacetate	641	641	15600	15600	38.1	0.55	0.00	1.372	6.081	0.371	0.401
9	acetone	635	635	15748	15748	42.2	0.71	0.08	1.359	20.560	0.361	0.568
10	DMF	638	638	15674	15674	43.8	0.89	0.00	1.428	36.710	0.409	0.550
11	DMSO	637	637	15699	15699	45.1	1.00	0.00	1.479	46.450	0.442	0.526
12	acetonitrile	630	630	15873	15873	45.6	0.75	0.19	1.344	35.940	0.350	0.609
13	2-propanol	646	619	15480	16155	49.2	0.48	0.76	1.377	19.920	0.374	0.552
14	1-butanol	648	617	15432	16207	50.2	0.47	0.84	1.399	17.510	0.390	0.527
15	1-propanol	646	613	15472	16323	50.7	0.52	0.84	1.386	20.450	0.380	0.548
16	ethanol	645	610	15504	16393	51.9	0.54	0.86	1.361	24.550	0.363	0.577
17	triethyleneglycol	655	617	15267	16207	53.5	0.88	0.66	1.456	23.690	0.427	0.511
18	NMF	634	622	15772	16077	54.1	0.90	0.62	1.432	189.000	0.412	0.511
19	methanol	634	604	15772	16556	55.4	0.60	0.98	1.328	32.660	0.338	0.617
20	ethyleneglycol	637	603	15699	16584	56.3	0.92	0.90	1.432	37.700	0.412	0.549

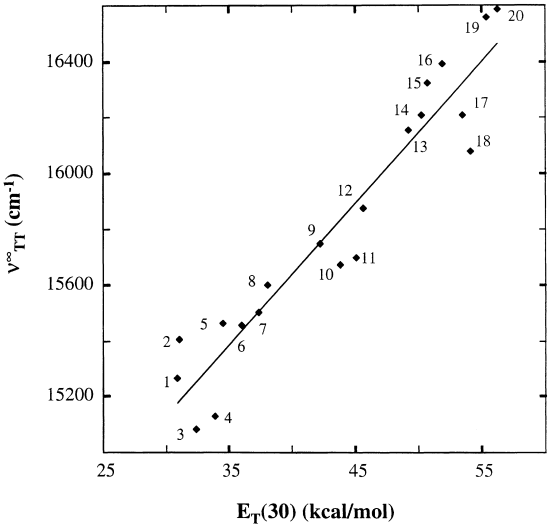

Fig. 3. ν_{TT}^∞ dependence on the empirical polarity parameter $E_T(30)$.

$$\nu_{TT}^\infty = (13600 \pm 200) + (51 \pm 4)E_T(30)$$
$$r = 0.952 \qquad n = 20 \tag{9}$$

Indeed, the solvatochromic comparative method (π^*, α, β) can enlighten us on the different interactions responsible for the T_1–T_n shift. Application of Eq. (8) to the data leads to the following multilinear regression

$$\nu_{TT}^\infty = (15340 \pm 40) + (340 \pm 70)\pi^* + (930 \pm 50)\alpha$$
$$r = 0.985 \qquad n = 18 \tag{10}$$

Toluene (aromatic) and CCl_4 (chlorinated) have been excluded (see the details of (π^*, α, β) method for justification [12]). The parameter β revealed to be without any influence on ν_{TT}^∞ in agreement with the fact that thioxanthone can accept hydrogen bonding from solvent but is on the contrary unable to act as an hydrogen bonding donor towards the solvent.

The ratio between the two coefficients a and s from Eq. (8) (numerical values Eq. (10)) in nearly 3 which means that the specific interactions are three-times more efficient than the normal solute/solvent interactions in shifting the T_1–T_n spectrum. This fact will be of interest in the discussion concerning the solvation dynamics.

3.2. *Unrelaxed* ^{3}TX *solvatochromy* (ν_{TT}^0)

We readily concede that the determination of ν_{TT}^0 is not straight forward. This is due to (i) the overlap of the S_1–S_n and T_1–T_n contributions and (ii) to the fact that the growing up of the triplet is concomitant to the shift of λ_{TT}^{max}. Therefore, the ν_{TT}^0 values are obtained only by extrapolation to both time and T_1–T_n absorption being 0. Fortunately, the S_1 lifetimes are known [8] which enable us to sufficiently disentangle the T_1–T_n from the S_1–S_n absorptions.

A first inspection of Table 1 does not reveal any clear trend of ν_{TT}^0 with the overall polarity. In fact the solvents used in this study have not only very different physical/chemical properties, but also quite different characteristic relaxation times (cf Table 2). It is, therefore, convenient to define, at least, three classes of solvents:

I Nonpolar solvents: cyclohexane, n-hexane, toluene and CCl_4
II Polar but nonhydroxylic solvents: dioxane, ether, THF, ethlyacetate, acetone, DMF, acetonitrile, and DMSO
III Polar and hydroxylic solvents: all the alcoholic solvents, and NMF

Table 2
Relaxation times (ps) of some probes and solvents. τ_D: No. 13, 15, 16, 19 from [25]; No. 10, 11, 12, 18 from [26]; No. 7, 9, 14 from [17], and No. 20 from [27]

No.	Solvent	Probes					Solvent		
		T–T absorption	Fluorescence						
		TX	C153 [16]			MPQB [17]			
		τ_{TX}	τ_3	τ_4	$\langle\tau\rangle$	τ_H	τ_D	$\tau_L=(\epsilon_\infty/\epsilon_0)\tau_D$ [14]	$\tau_M=(2\epsilon_0+\epsilon_\infty)/(3\epsilon_0 g_k)\ \tau_D$ [14]
5	Ether	–							
6	Dioxane	–	2.21	18.30	1.70				
7	THF	–	0.228	1.52	0.94		3	0.8	2
9	Acetone	–	0.187	1.09	0.58		3	0.3	2
10	DMF	–	1.7	29.10	2.00		10	0.6	6
11	DMSO	–	2.29	10.70	2.00		21	1.0	13
12	MeCN	–	0.089	0.63	0.26		3	0.2	2
13	2-propanol	95					359	35.1	114
14	1-butanol	120	42.6	133.00	63.00		528	58.1	158.03
15	1-propanol	90	6.57	47.80	26.00		329	30.9	101
16	ethanol	72	5.03	29.60	16.00	41	163	12.4	52
17	triethyleneglycol	210							
18	NMF	55	3.42	53.40	5.70		128	1.4	37
19	methanol	20	3.2	15.30	5.00	<40	52	2.8	16
20	ethyleneglycol	80	4.98	32.00	15.30	52	105	5.1	31

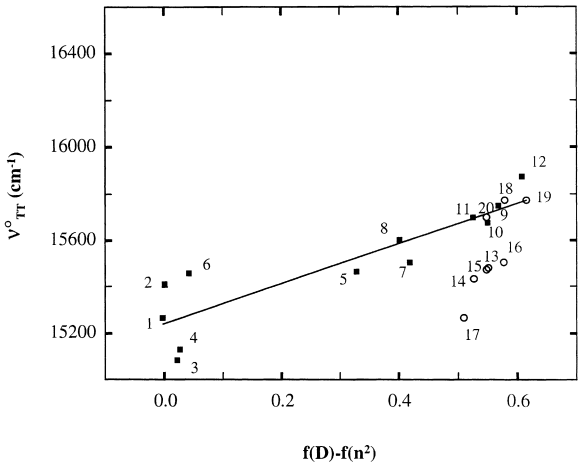

Fig. 4. Comparison between the ν^0_{TT} (equal to ν^∞_{TT}) of nonpolar/polar solvents (■ and ν^0_{TT} of hydroxylic solvents (○). The line is the same than the one reported in Fig. 2.

The first two classes contain solvents for which the relaxation times are very short: the longitudinal relaxation time τ_L is less than 2 ps, shorter than our time resolution of 10 ps. Thus, for these two classes of solvents (I and II), we are only able to observe the equilibrium between the solute, TX, and the solvent: all classical electrostatic interactions (dipolarity/polarisability) are effective. For the solvents contained in the third class, the problem is quite different. Indeed, it is necessary to subdivise this class: (i) III_s containing the 'slow hydroxylic solvents', for which relaxation times τ_L are longer than 10 ps (1 and 2-propanol, 1-butanol, triethyleneglycol, and ethanol), (ii) III_f containing the 'fast hydroxylic solvents', for which relaxation times τ_L are shorter than 10 ps (methanol, ethyleneglycol and NMF).

In Fig. 4, the ν^0_{TT} of fast (III_f) (No. 18, 19, 20) and slow hydroxylic (III_s) (No. 13–17) solvents are displayed with the ν^0_{TT} of solvents of Classes I and II (No. 1–12) It should be noted that for solvents No. 1–12, ν^0_{TT} and ν^∞_{TT} are identical (cf Table 1). It can be seen that these 'fast' hydroxylic solvents satisfy very well to the linear regression (which represents the situation when dipolar interactions are effective), indicating that, in these three solvents, classical dipolar interactions are really effective. On the opposite, the ν^0_{TT} of slow hydroxylic solvents (No. 13–17) do not correlate with the other solvents, and moreover are lower than expected, indicating that in these 'slow' solvents classical dipolar interactions are not effective.

Thus, in the solvents of the Classes II and III_f we observe an equilibrium state between TX and solvents molecules, where all classical dipolar and polarisabilities interactions are effective (but not the specific interactions). On the opposite, in the solvents of the Class I, which contains nonpolar solvents, only the electronic polarisability of the solvent can play a role in the solvation of TX. It is quite the same in the solvents of the Class III_s, in which dipolar interactions are not fast enough to relax before the measurement of ν^0_{TT}. For these two later classes, neither the dielectric constant (D) nor the dipolarity/polarisability interactions (π^*) or the specific interactions (α) can play any role in the values of ν^0_{TT}. Therefore, the term $f(D)$ in relation Eqs. (3)–(5) drops out, and, as a consequence, the solvatochromism of TX should depend only on the electronic polarisabilities of the solvents (as to say on the Onsager's refractive index function of the solvents). This is confirmed by Fig. 5 where ν^0_{TT} depends linearly on the $f(n^2)$ function.

$$\nu^0_{TT} = (17100 \pm 300) - (4500 \pm 700)\, f(n^2)$$
$$r = 0.928 \qquad n = 9 \tag{11}$$

As a general rule, polarisabilities in the excited states are larger than in the ground states ($\alpha_e > \alpha_g$). Moreover, from the

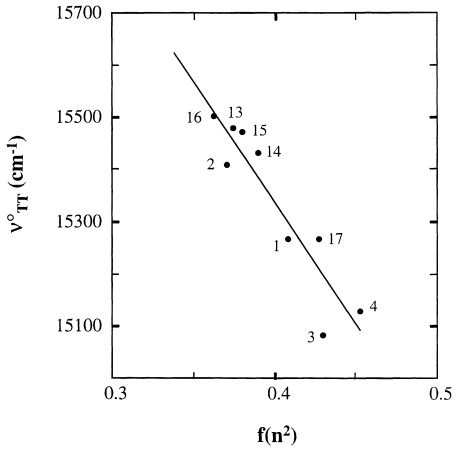

Fig. 5. Linear correlation between ν^0_{TT} and $f(n^2)$.

study on ν^∞_{TT} it appears that $\mu_e < \mu_g$. Thus, as $f(n^2)$ increases, it can be deduced from Eqs. (3)–(6) that ν^0_{TT} should undergo respectively a red (3), a blue (4), a blue (5) and then a red (6) shift. It seems rather unreal to compute these four contributions to the overall shift due to the lack of data concerning a, L, C, α_e, α_g. In this context, it is important to become aware of the fact that Eqs. (3)–(6) proved to be very useful for describing solvent effects on electronic transitions from a relaxed initial state to a Franck–Condon final state. It is not the case in this work since ν^0_{TT} corresponds to a transition from T_1 (not totally relaxed) towards an upper state T_n (Franck–Condon state).

3.3. Time evolution of the shift of the T–T absorption

The solvatochromy of the unrelaxed ν^0_{TT} and relaxed ν^∞_{TT} triplet state being explained, it is instructive to investigate the kinetics of the relaxation $\nu^0_{TT} \rightarrow \nu^\infty_{TT}$ and its solvent dependence. Fig. 6 shows the 3D contour plot of the T–T absorption in 1-butanol, and it can be seen that the time dependence of the shift occurs on nearly 100 ps. Such time dependence of the relaxation process is usually described with the solvation time correlation function $C(t)$ which can be written in our case $C(t) = (\nu^t_{TT} - \nu^\infty_{TT})/(\nu^0_{TT} - \nu^\infty_{TT})$. The fit of this experimental function to (i) monoexponential, (ii) sum of monoexponential or (iii) nonexponential functions is one of the major task of solvation dynamics. Most of the experimental information was obtained until now from the dynamic Stokes shift of a fluoro probe, i.e., a probe in its singlet excited state. Among these, Coumarin 153 (C 153) was largely investigated and a large body of data was recently published [17] showing the great complexity of the solvation dynamics of this probe. The authors have to introduce a sum of up to four exponential functions (i.e., up to four relaxation times) in order to describe the kinetics of solvent response following the excitation of the C153 probe. The paper [18] reports that this probe is sensitive to nondipolar solvent like benzene, which proves that quadrupolar interactions may play a role in the dynamics of solvation. It is worth to note that this probe was classified as insensitive toward H-specific interactions. On the opposite, for another solute, MPQB [19], specific interactions revealed to play an important role in the solvation dynamics. With this later one, it was possible to measure the formation time of the specific interaction between solute and solvent: mainly the importance of hydrogen bond formation in the relaxation time of solvent was pointed out, leading to longer relaxation times than predicted by the continuum model. A recent paper [20] concerning the solvation dynamics of three different coumarins shows that the breaking/formation of hydrogen bonding could also be responsible for ultrafast relaxation time of fluoroprobe.

Inspection of the literature reveals that the observed solvation dynamics are not simply related to the relaxation time of the solvents. It can be, however, instructive to consider the set of usual solvent characteristic times. In the case of the classical dielectric continuum model, the solvent is characterized by its bulk frequency dependent dielectric function $\varepsilon(\omega)$. For liquids having a single Debye type dielectric dispersion, this theory predicts that solvent molecules should monoexponentialy relax with a time constant equal to the longitudinal relaxation time $\tau_L = (\varepsilon_\infty/\varepsilon_0)\tau_D$ [21–23], where ε_0 and ε_∞ are the static and infinite frequency dielectric constants and τ_D is the Debye relaxation time (or the bulk dielectric relaxation time) determining the frequency dielectric function $\varepsilon(\omega) = \varepsilon_\infty + (\varepsilon_0 - \varepsilon_\infty/1 + i\omega\tau_D)$. The relaxation time τ_L is a bulk property which involves the response of many solvent molecules correlated to each other.

Recently, a microscopic (single particle) reorientation time, τ_M, of the solvent molecules was determined [24]. In this approach, two cases must be considered. On one hand it is assumed that far from the solute, the dipolar solvent is

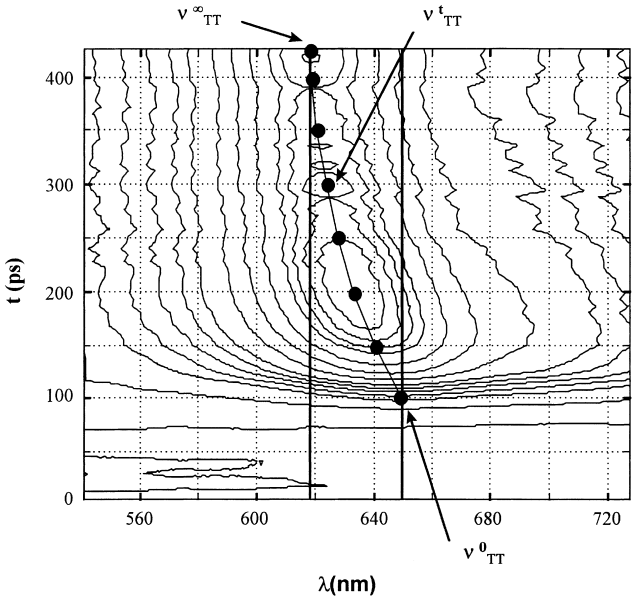

Fig. 6. The 3D contour plot of the T–T absorption spectrum of thioxanthone (TX) in 1-butanol.

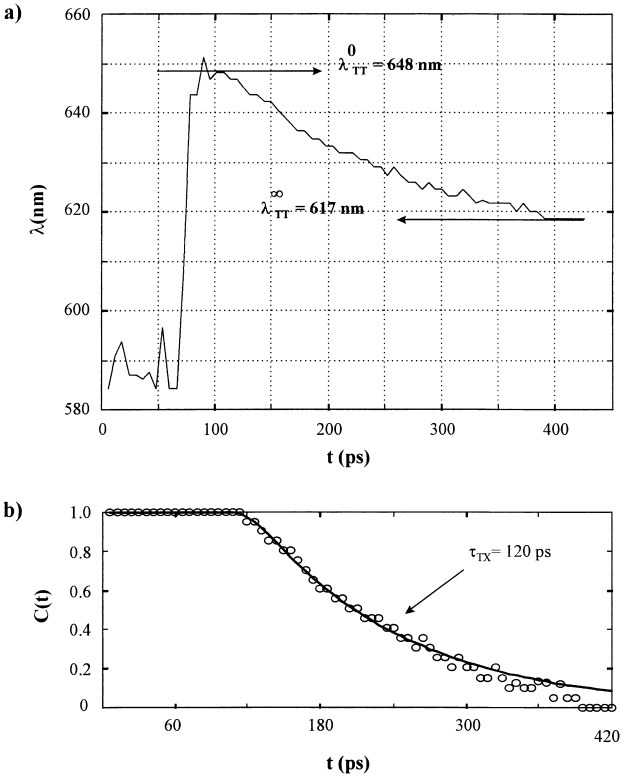

Fig. 7. Time evolution of the T_1–T_n shift in 1-butanol: (a) time dependence of the shift; (b) monoexponential fit according to the $C(t)$ function.

considered as a continuum, and thus the solvent molecules relaxe with a time constant equal to τ_L. On the other hand, near the probe molecule, the interaction between solute and solvent could be so important that the correlation between solvent molecules gets broken and thus the solvent molecules individually relax with a characteristic time equal to τ_M, defined as $\tau_M = (2\varepsilon_0 + \varepsilon_\infty) / (3\varepsilon_0 g_k)\, \tau_D$ where g_k is the Kirkwood factor. The value of this parameter indicates to which extent the solvent molecules align themselves with respect to their neighbours, and is an index of short range order in the liquid. For nonassociated solvents, this factor is nearly equal to unity, but in associated solvents such as hydroxylic solvents, g_k is greater than unity and was taken here equal to 3 [19].

In Fig. 7(a) the time dependent maximum of absorption of the T–T transition in 1-butanol is displayed. It can be seen that the maximum of absorption evolves with time going from λ^0_{TT} (red) to λ^∞_{TT} (blue) indicating a stabilization of the lowest triplet by solvent reorientation. Then the $C(t)$ function was calculated and used to determine the characteristic time of the relaxation process. As an example, a monoexponential decay was found for TX in 1-butanol with a relaxation time $\tau_{TX} = 120$ ps as shown in Fig. 7(b). Moreover, all our experiments could be fitted using a monoexponential decay and the corresponding relaxation times are reported in Table 2. Also, other relaxation times like τ_M, τ_L, τ_D already defined, τ_H time of hydrogen bonding are reported in Table 2 as well as τ_3, τ_4 and $\langle\tau\rangle$ from the work of Maroncelli and co-workers [17] (here τ_3, τ_4 are the two longer relaxation times for each solvent, and not the ones defined by the authors in the article [17]). These times are representative of the specific interaction under our interest.

Inspection of Table 2 reveals that our experimental values τ_{TX} are in good agreement with the microscopic time τ_M of the solvent and/or with the times τ_H reported for the probe MPQB sensitive to hydrogen bonding. Here τ_H represents the formation time of hydrogen bond between solute and solvent molecules. As it was already said, for this probe, it was possible to determine the hydrogen bond formation time (τ_H) which is a single molecular process significantly longer than the bulk response of the solvent (τ_L).

On the other hand, the relaxation times concerning C 153, which is not affected by specific interactions, significantly differ from τ_{TX}. The characteristic times found in the literature (τ_3, τ_4 and $\langle\tau\rangle$ in Table 2) where τ_3 and τ_4 are the two longer relaxation times obtained with C153, while $\langle\tau\rangle$ is the average relaxation time, taking into account all the other relaxation times and are much more smaller than our results. These results agree much better with the longitudinal relaxation time τ_L, showing that the major process of solvent relaxation molecules is governed by the bulk dielectric response of the solvent.

The dipolar moment of ^{3}TX($\mu_{T1} = 4.9$ D) is lower than the dipolar moment of C153 ($\mu_{S1} \sim 15$ D). Then the dipolar interaction between ^{3}TX and solvent would be weaker than in the case of C153. As for C153 the relaxation times are governed by the bulk dielectric response τ_L, we could expect that for ^{3}TX solvent reorganization would behave identically. However, we have shown that the solvation times around ^{3}TX are slightly longer than the molecular relaxation times of the solvents τ_M, and the H-bond formation time of MPQB τ_M. This might be significant of a strong interaction between ^{3}TX and solvent, leading to as lower single molecular relaxation time.

It is proposed therefore that the relaxation of the solvent molecules around ^{3}TX is governed by a short range interaction (τ_M) exhibiting a hydrogen bond nature (τ_H). This result is in line with the remark concerning the three time higher contribution of the specific interactions compared to the dipolar interactions in the shift of ν^∞_{TT} (cf. Eq. (10)). Thus, specific interactions play a key role in all the facets of the photophysic of thioxanthone: fluorescence lifetime, solvatochromic shifts and intersystem crossing rates k_{ISC} [28].

4. Conclusions

Time resolved absorption of thioxanthone in its triplet state (^{3}TX) was investigated in different solvents. It has been shown that relaxed $^3\mathrm{TX}\left(\nu^\infty_{TT}\right)$ and unrelaxed $^3\mathrm{TX}\left(\nu^0_{TT}\right)$ undergo shifts which are governed respectively by dipolar/specific and polarisability interactions. Moreover, the time evolution of the shift in a given alcohol is

monoexponential. Comparison of these relaxation times τ_{TX} $\left(\nu_{TT}^{0} \rightarrow \nu_{TT}^{\infty}\right)$ obtained in alcohols with those of other probes (C153, MPQB) and with the solvent's characteristic relaxation times, reveals the role of the hydrogen bonding, at a microscopic level, in the solvation dynamics of ^{3}TX. Indeed, it was possible to estimate the formation time of an hydrogen bond between the solute ^{3}TX and the solvents molecule. Thioxanthone is certainly not a passive reporter of what is going on in its surroundings.

Acknowledgements

We thank the "Région Alsace", "Département du Haut-Rhin" and the "Ville de Mulhouse" for their financial support in the development of the picosecond pump-probe experiment.

References

[1] P. Suppan, J. Photochem. Photobiol. A: Chem. 50 (1990) 293.
[2] P. Suppan, Solvatochromism, The Royal Society of Chemistry, Ed., 1997
[3] J.C. Dalton, F.C. Montgomery, J. Am. Chem. Soc. 96 (1974) 6230.
[4] T. Lai, E.C. Lim, Chem. Phys. Lett. 73 (1980) 244.
[5] T. Lai, E.C. Lim, Chem. Phys. Lett. 84 (1981) 303.
[6] K.A. Abdullah, T.J. Kemp, J. Photochem. 32 (1986) 49.
[7] D. Burget, P. Jacques, J. Chim. Phys. 88 (1991) 675.
[8] D. Burget, P. Jacques, J. Lumin. 54 (1992) 177.
[9] N. Tamai, T. Asahi, H. Masuhara, Chem. Phys. Lett. 198 (1992) 413.
[10] S.L. Murov, I. Carmichael, G. Hug, Handbook of Photochemistry, Marcel-Dekker, New York, 1993
[11] C. Reichardt, Solvents and Solvent Effects in Organic Chemistry, VCH, 1988
[12] M.J. Kamlet, J.L.M. Abboud, M.H. Abraham, R.W. Taft, J. Org. Chem. 48 (1983) 2877.
[13] Y. Marcus, Chem. Soc. Rev. 409 (1993)
[14] R.M.C. Gon Calves, A.M.N. Simoes, L.M.P.C. Albuquerque, M. Roses, C. Rafols, E. Bosch, J. Chem. Res. (S) 214 (1993)
[15] J.A. Riddick, W.B. Bunger, T.K. Sakano, Organic Solvents, Wiley, 1986
[16] H. Lumbroso, J. Cure, M. Evers, Z. Naturforsch. 41a (1986) 1250
[17] M.L. Horng, J.A. Gardecki, A. Papazyan, M. Maroncelli, J. Phys. Chem. 99 (1995) 17311.
[18] L. Reynolds, J.A. Gardecki, S.J.V. Franklard, M.L. Horng, M. Maroncelli, J. Phys. Chem. 100 (1996) 10337.
[19] A. Declemy, C. Rulliere, P. Kottis, Laser Chem. 10 (1990) 413.
[20] T. Gustavsson, L. Cassara, V. Gulbinas, G. Gurzadyan, J.C. Mialocq, S. Pommeret, M. Sorgius, P. Van Der Meulen, J. Phys. Chem. A 102 (1998) 4229.
[21] G. Van Der Zwan, J.T. Hynes, J. Phys. Chem. 89 (1985) 4181.
[22] E.W. Castner Jr., M. Maroncelli, G.R. Fleming, J. Chem. Phys. 86(3) (1987) 1090.
[23] B. Bagchi, D.W. Oxtoby, G.R. Fleming, Chem. Phys. 86 (1984) 257.
[24] P. Madden, D. Kivelson, Adv. Chem. Phys. 56 (1984) 467.
[25] J. Barthel, K. Bachhuber, R. Buchner, H. Hetzenauer, Chem. Phys. Letters 165 (1990) 369.
[26] J. Barthel, K. Bachhuber, R. Buchner, J.B. Gill, M. Kleebauer, Chem. Phys. Letters 167 (1990) 62.
[27] G.B. Dutt, S. Doraiswamy, N. Periasamy, B. Venkataraman, J. Chem. Phys. 93(12) (1990) 8498.
[28] P. Jacques, C. Ley, F. Morlet-Savary, J.P. Fouassier, to be published.